2. N. V. Belan, V. I. Kiryushko, and N. A. Mashtylev, "The current distribution in a coaxial accelerator," Zh. Tekh. Fiz., 40, No. 1 (1970).
3. A. A. Kalmykov, "Pulsed plasma accelerators," in: Physics and Applications of Plasma Accelerators [in Russian], Nauka i Tekhnika, Minsk (1974).
4. P.E. Kovrov and A. P. Shubin, "High-current coaxial accelerator in the quasistationary mode," in: Physics and Applications of Plasma Accelerators [in Russian], Nauka i Tekhnika, Minsk (1974).
5. K. V. Brushlinskii and A. I. Morozov, "Calculation of two-dimensional plasma flows in channels," in; Problems of Plasma Theory [in Russian], No. 8, Atomizdat, Moscow (1974).
6. K. V. Brushlinskii, A. I. Morozov, V.V. Paleichik, and V. V. Solov'ev, "Calculation of compression plasma flows in coaxial channels," Fiz. Plazmy, 2, No. 4 (1976).
7. N. V. Belan, S. I. Zabara, N. A. Mashtylev, and A. I. Morozov, "Calculation of the two-dimensional nonstationary isothermal plasma flow in a coaxial channel," in: Proceedings of the Second All-Union Conference on Plasma Accelerators, [in Russian], Minsk (1973).
8. N. V. Belan, N. A. Mashtylev, and L. V. Shushlyapin, "Two-dimensional motion of a heat-conducting plasma in a pulsed accelerator," in: Proccedings of the Second All-Union Conference on Plasma Accelerators, [in Russian], Minsk (1973).
9. N. V. Belan, N. A. Mashtylev, and S. I. Zabara, "Calculation of two-dimensional nonstationary plasma flow in coaxial channels," in: Low-Temperature Plasma Sources [in Russian], No. 1, Izd. KhAI, Khar'kov (1975).
10. I. S. Berezin and N. P. Zhidkov, Computational Methods [in Russian], Fizmatgiz, Moscow (1959).
11. N. V. Belan, N. A.Mashtylev, B. I. Panachevnyi, and L. V. Shushlyapin, "Effect of the distribution of the elements in a capacitive energy store on the form of the current in a pulsed plasma injector," Zh. Tekh. Fiz., 43, No. 6 (1974).

INVESTIGATION OF SLIDING SPARK IN AIR

S.I. Andreev, E. A. Zobov, and A. N. Sidorov

UDC 533.9+518.5+537.517

Sliding sparks occur on the surface of a dielectric under whose layer there is a conductor [1]. They appear especially easily if this conductor (we henceforth call it the initiator) is electrically connected to one of the electrodes.

Extensive literature (for instance, [1-8]) is devoted to the study of sliding sparks. Mainly the conditions for the origination of such discharges in high-voltage techniques have been studied. Questions on the dynamics of development have been investigated in [7, 8]. These investigations refer to the domain of comparatively small gaps ($l \leq 0.24$ m).

The present paper is devoted to an investigation of the physical processes for the development of sliding sparks from short to long (8 m) gaps.

METHODOLOGY OF THE EXPERIMENT

Sliding sparks occurred on the surface of thin-film dielectrics covered either with thin metal surfaces or tubes. A voltage being formed during the discharge of a condenser battery with $C = 0.5-16$ μF (Fig. 1a) through a controllable discharger 1 on the primary winding (one turn) of a cable transformer 2 was used in the research. A voltage in the form of a damped cosinusoid with a period of 2-18 μsec (a logarithmic damping decrement of ~0.01) occurred at the secondary winding (ten turns). This voltage was applied to the electrodes of the discharge gap (DG) under investigation. An oscillogram was made by using the divider D_0. The maximum value was determined by using a ball 3 of diameter 380 mm (the calibration tables were taken from [5]).

The current distribution was measured along the length of the channel (Fig. 1b). To do this, the initiator 4 was fabricated from mutually insulated flat metal plates. The current shunts Sh permitted taking oscill-

Leningrad. Translated from Zhurnal Prikladnoi Mekhaniki i Tekhnicheskoi Fiziki, No. 3, pp. 38-43, May-June, 1978. Original article submitted December 23, 1976.

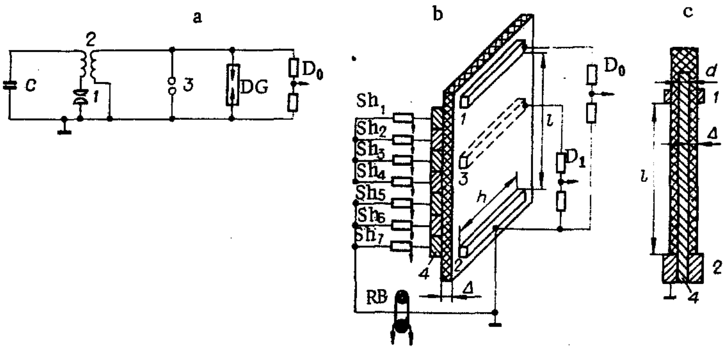

Fig. 1

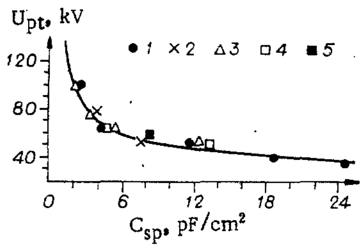

Fig. 2

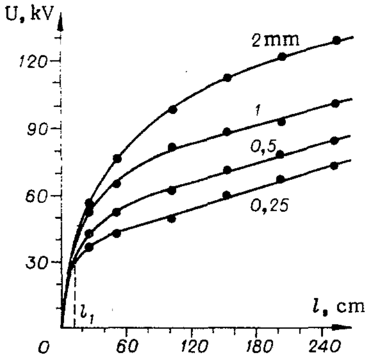

Fig. 3

ograms of the plates. The Rogowski belt (RB) measured the total current. The initiator was connected to the grounded electrode 2. The discharge always started from the side of the high-voltage electrode 1.

The voltage distribution along the length of the gap was measured by the probing electrode 3 and the voltage divider D_1 (Fig. 1b).

Development of the body of the discharge channel flow was recorded by using a high-speed photorecorder (SFR). The scan was carried out perpendicularly to the channel axis. Development of the channel was investigated at different spacings from the electrodes. Special measures were taken to stabilize the channel in space. To do this, a narrow (1 mm wide) control strip of polystyrene lacquer with a suspended powder of barium oxide (95%) and graphite (5%) was deposited on the surface. The method of controlling the development of the sliding sparks is examined in [9].

The length of the discharge gap l in a plane structure (see Fig. 1b) varied between 12 and 140 cm and in the cylindrical structure (Fig. 1c) between 25 and 800 cm. The width of the discharge gap in the plane structure h was 12 or 32 cm and in the cylindrical structure πd, with diameter $d = 4$ cm.

The following dielectric films were used: polyethylene (with a relative dielectric permittivity $\varepsilon = 2.2$), polyethylene terefluorate ($\varepsilon = 3.2$), cellulose triacetate ($\varepsilon = 3.5$), fluoroplastic mark 23 ($\varepsilon = 7.8$) and mark F26 ($\varepsilon = 10.3$), sheet vinyl plastic ($\varepsilon = 3.1$0, and cardboard ($\varepsilon = 4 \div 6$). The thickness of the dielectric coatings Δ varied within broad limits.

The minimal voltage at which punchthrough (electrical breakdown) occurs depends mainly on l, Δ, and ε [5]. Investigations of the punchthrough voltage U_{pt} of the dielectric parameters (Fig. 2) for a large gap length ($l = 1$ m) showed that a dependence on the ratio ε/Δ exists, but not on ε and Δ separately. Different points have been obtained in Fig. 2 by using dielectric materials with different values of the thickness Δ and dielectric constant ε (the points 1 in Fig. 2 have been obtained for polyethylene, 2 for Lavsan (Dacron)m 3 for cellulose triacetate, 4 for fluoroplastic F-23, and 5 for fluoroplastic F-26).

Therefore, the capacitance of the dielectric film ($C_{sp} = 0.88\ \varepsilon/\Delta$ pF/cm^2 if Δ is in millimeters) is the governing factor in the punchthrough of long ($l \gtrsim 1$ m) discharge gaps by a sliding spark, and the influence of the dielectric material enters only in terms of the physical quantity ε. An especially strong effect of C_{sp} on U_{pt} occurs in the range of variation of C_{sp} between 0.5 and 5 pF/cm^2. A further increase in U_{sp}(above 5 pF/cm^2) does not result in any noticeable diminution in the quantity U_{pt} (see Fig. 2). This can be explained by the fact that the growth of the capacitive current influencing the channel conductivity does not result in a diminution in the voltage drop in the channel. This drop turns out to be sufficiently small and the potential of a high-voltage electrode with low losses is transferred to the head. Consequently, a self-consistent mode occurs in which the electrical field intensity in the head is maintained high during the time of discharge development. The magnitude of C_{sp} at which this mode occurs determines the magnitude of the critical length l_{cr}.

Now let us examine the dependence of the punchthrough voltage on the length (Fig. 3) (the magnitude of the dielectric thickness in millimeters is shown near the curves, and the dielectric constant $\varepsilon = 3.2$-3.5). As is seen from the results in Fig. 3, the curve $U_{pt}(l)$ can be divided into three parts.

The first section $l \leq l_1$ has a value of the punchthrough voltage which differs slightly from the corresponding value of the volume punchthrough of a gas under the conditions of pointed electrodes ($U_{pt}/l = E_1 = 300 \div 350$ kV/m). There is no influence of the material in this section. However, the boundary of the first section l_1 depends on ε/Δ. As an analysis of experimental results has shown, the gap length at which punchthrough differs slightly from the volume value is determined by the formula

$$l_1 \approx 0.045\, C_{sp}^{-0.5} + 0.12\ \text{m};\ U_{pt_1} = E_1 l$$

(C_{sp}, pF/cm^2).

The second section $l_1 \leq l \leq l_{cr}$ is usually studied by means of sliding discharges in the literature [1-8]. Under our conditions the punchthrough voltage is determined by the formula

$$U_{pt_2} = U_{pt_1} + (U_{cr} - U_{pt_1})\sqrt{\frac{l - l_1}{l_{cr} - l_1}},$$

where U_{cr} and l_{cr} are the values of the punchthrough voltage and the length at the boundary between the second and third sections. Intersections of the curves with straight lines correspond to them on the curve $U_{pt}(l)$. It has been established experimentally that U_{cr} and l_{cr} are single-value functions (for a given mode of voltage) of C_{sp}.

$$l_{cr} = 1{,}8 C_{sp}^{-0.5}\text{,m},\quad U_{cr} = 130 C_{sp}^{-0.5}\text{, kV},$$

if C_{sp} is in pF/cm^2.

The second section is the transition region from a discharge in a volume to a "purely" surface discharge. This latter is characterized by the governing role of the capacitive current through the initiator. The magnitude of the current in the channel grows with the passage to a "purely" surface discharge, but the channel resistance drops. The electrode potential is hence transferred to the region of the channel head to a considerable extent, thereby determining the intensity of the ionization processes at the head. It is essential that the nature of the ionization processes vary weakly as the discharge channel develops. Such a development is self consistent: The intensity of the ionization processes is determined by the magnitude of the potential in the head, and the magnitude of this potential is determined by the channel conductivity, which depends on the intensity of the ionization processes. In this case the governing parameter of the process is the field intensity in the channel E_3.

The punchthrough voltage in the domain of the third section can be determined from the formula

$$U_{pt} \approx 1.1\,[U_{cr} + E_3(l - l_{cr})]. \quad (1)$$

Under the conditions of this experiment, $E_3 = 14 \pm 1.5$ kV/m. The error which (1) yields does not exceed 15-20%, if $l \leq 6$ m. For $l > 6$ m, E_3 should take the value 10 kV/m.

Punchthrough of gaps of long length occurs for $U = U_{pt}$, as a rule, during several half-periods in the whole range of frequencies used (30-300 kHz). The use of the results presented above when working with an undamped alternating voltage in the same frequency range should not result in noticeable differences. In order to break through a gap in a shorter time, the magnitude of the applied voltage must increase compared to the U_{pt} determined by (1).

PUNCHTHROUGH DEVELOPMENT

If the amplitude of the applied voltage equals U_{pt}, then, as a rule, punchthrough occurs by one channel although there are several channels being developed in parallel in the incomplete stage. In the presence of an overvoltage, punchthrough can occur simultaneously by several channels. The number of such channels grows with the rise in the overvoltage and rapidly reaches a maximum. The criteria for reaching the maximum number of channels are different for $l < l_{cr}$ and $l > l_{cr}$. For $l < l_{cr}$ this number is directly independent of the overvoltage and is determined uniquely by the condition

$$U = 1.3\, U_{cr} \quad \text{for} \quad l < l_{cr}. \quad (2)$$

For $l_1 \leq l \ll l_{cr}$, condition (2) corresponds to a high overvoltage, and for $l \approx l_{cr}$ a 30% overvoltage is sufficient. This same magnitude of the overvoltage is even conserved for $l > l_{cr}$.

$$U = 1.3\, U_{pt} \quad \text{for} \quad l > l_{cr}. \quad (3)$$

Here $U_{pt} > U_{cr}$. This is related to the fact that for $l > l_{cr}$ incomplete channels possess high conductivity and condition (3) is required only to increase the synchronization of their closure of the discharge gap.

It is interesting that the effect of suppression of one channel by another exerts a governing influence on the instantaneous length of the incomplete channel and not on the "current-collecting" surface. It is seen in Fig. 4a that the central channel delayed the development of the neighbors and "seized" the whole "current-collecting" surface. The size of the discharge gap in Fig. 4 is $l = 62$ cm, h = 32 cm, while the dielectric thickness is 1 mm. A 60 kV voltage is applied in Fig. 4a, b and a 120 kV voltage in Fig. 4c. It is seen from Fig. 4b that the central channel being developed between the other two has the same length (rate of development) as the side channels with the unbounded "current-collecting" surface on one side. This surface only determines the brightness of the glow and the conductivity of the channel. However, the number of incomplete channels depends on the "current-collecting" surface. The fact is that after the discharge gap has been closed, the current grows sharply and the voltage on it drops because of the rise in the inductive drop in the outer loop. Hence, a weakly conducting channel can be "quenched" (see Fig. 4c). Associated with this is the dependence of U_{pt} on the width h of the surface, which holds for h (or πd) less than 10 cm.

The rate of channel development is not constant. Pauses associated with fluctuations in the applied voltage have been observed in the channel development. In Fig. 5 photographic sweeps of the leader channel at the frequencies 55 kHz (a) and 250 kHz (b) are presented. The whole 40-cm-long gap is represented in the frame. The voltage is 60 kV. The mean rate of channel development along the gap is $\sim 5 \cdot 10^7$ cm/sec, while

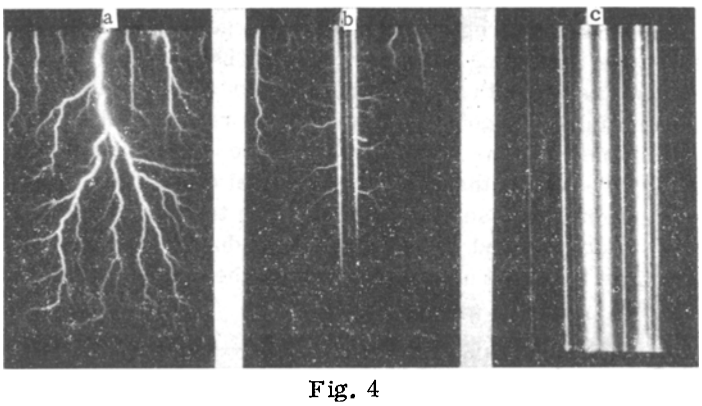

Fig. 4

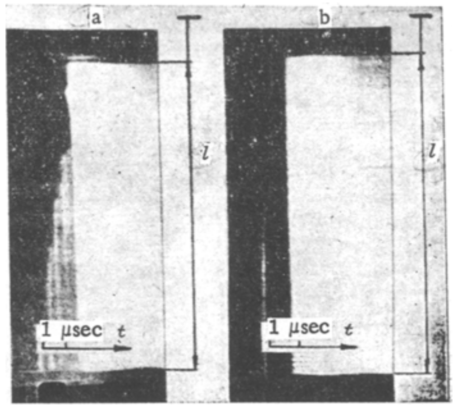

Fig. 5

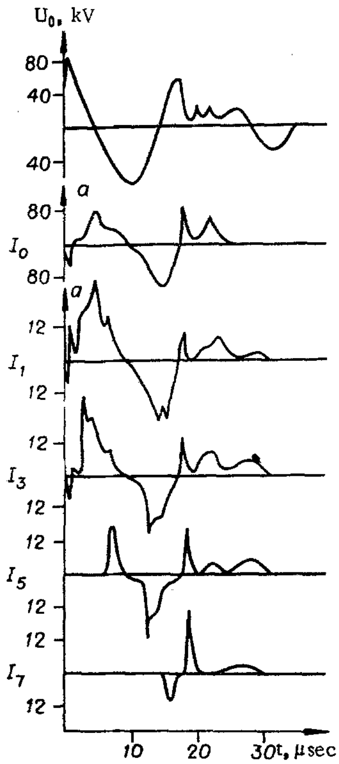

Fig. 6

the rate between the pauses is at least an order of magnitude higher. Pauses have also been observed even in the voltage rise stage [9]. In our opinion, the origin of these pauses is associated with the nonuniform distribution of the conductivity along the length. The hotter sections of the channel cool off more intensively during the pauses and the conductivity along the length is equilibrated. The electrode potential is transferred to the head and ionization processes again develop.

The origination of an opposing channel from the grounded electrode (see Fig. 5b) can also exert influence during punchthrough. The probability of the origination of an opposing channel rises with the rise in the frequency.

Now let us examine the nature of the change in channel conductivity during its development. Oscillograms of the currents through the separate initiator sections (I_1, I_3, I_5, I_7) and their sum – the total current (I_0) – are presented in Fig. 6. The gap length was 140 cm; the amplitude of the applied voltage was 55 kV. Also presented here is an oscillogram of the voltage U in the gap. The current through the initiator has two components: $i = C\partial U/\partial t + U\partial C/\partial t$. Since the voltage has the form of a cosinusoid, then the current component

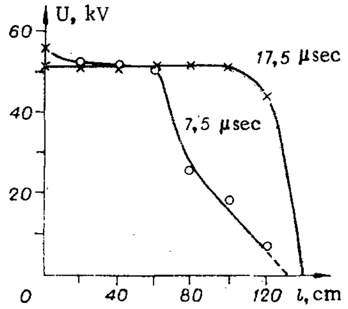

Fig. 7

i ~ ∂U/∂t has a characteristic overshoot at the voltage pulse front. The complex nature of the change in capacitance governed by the irregular development of ionization processes results in the complex form of the current oscillogram (there is no influence of adjustments on the oscillograms in Fig. 6).

The potential distribution at the time of punchthrough (t = 17.5 μsec) and at an earlier time (7.5 μsec) is shown in Fig. 7. These distributions correlate with the current oscillograms and permit a determination of the nature of the channel resistance distribution over its length. Thus, for instance, when the channel reaches the length $l = 120$ cm (for $l_{cr} = 105$ cm) at the time t = 7.5 μsec, the following resistance distribution would hold: For a high-voltage electrode ($l = 0$) the resistance per unit length is $R/l = 70$ Ω/cm; in the range $20 \leq l \leq 80$ cm the value is $R/l = 14$ Ω/cm [the conductivity is hence $\sigma = 2(\Omega \cdot cm)^{-1}$]; and in the region of the channel head $60 \leq l \leq 80$ cm, the value of R/l grows to 1000 Ω/cm. The resistance drops for still greater lengths. This is related to the propagation of the opposing channel observed on the SFR photogram. The channel resistance undergoes significant changes during the development process.

Using the dependence of the velocity of directed electron motion on the field intensity, we obtain the value of the electron concentration in the channel of an incomplete leader of 1 m length $n_e = 10^{14}$–10^{15} cm^{-3}[this corresponds to a conductivity on the order of units $(\Omega \cdot cm)^{-1}$ in a 50-100-V/cm field]. In a completed discharge channel, the electron concentration is 1-2 orders of magnitude higher.

LITERATURE CITED

1. R. Toepler, "Stosspannung Überschlag und Durchschlag bei Isolation," Elektrotech. Z., 45, 1045 (1924).
2. R. Stregel, Elektrische Stossfestigkeit, 2nd ed., Springer-Verlag, Berlin (1955).
3. A. Roth, Hochspannungstechnik, Springer-Verlag, Berlin (1959).
4. P. N. Dashuk, S. L. Zaients, V. S. Komel'kov, G.S. Kuchinskii, N. N. Nikolaevskaya, P.I. Shkuropat, and G. A. Shneerson, Techniques of High Current Pulses and Magnetic Fields [in Russian], Atomzidat, Moscow (1970).
5. Taschenbuch Electrotechnik, Vol. 2, Verlag Technik, Berlin (1965).
6. V. L. Sirotinskii, High-Voltage Techniques [in Russian]. Gosénergoizdat, Moscow (1951).
7. A. I. Limasov and S. F. Pokrovskii, "Use of an image converter to investigate sliding discharges on the surface of solid dielectrics," Sibirsk. Nauchno-Issled. Inst. Elektrotekh., No. 10, 43 (1972).
8. V. S. Komel'kov and E. Z. Meilikhov, "Growth of negative Lichtenberg figures in a nanosecond time interval," Zh. Tekh. Fiz., 33, No. 8, 934 (1963).
9. S. I. Andreev, E. A. Zobov, and A. N. Sidorov, "Method of controlling the development and formation of a system of parallel sliding spark channels in air at atmospheric pressure," Zh. Prikl. Mekh. Tekh. Fiz., No. 3 (1976).